Effects of B cell–activating factor on tumor immunity

Mark Yarchoan, Won Jin Ho, Aditya Mohan, Yajas Shah, Teena Vithayathil, James Leatherman, Lauren Dennison, Neeha Zaidi, Sudipto Ganguly, Skylar Woolman, Kayla Cruz, Todd D. Armstrong, and Elizabeth M. Jaffee

Bloomberg–Kimmel Institute for Cancer Immunotherapy, Johns Hopkins University School of Medicine, Baltimore, Maryland, USA

Immunotherapies that modulate T cell function have been firmly established as a pillar of cancer therapy, whereas the potential for B cells in the antitumor immune response is less established. B cell–activating factor (BAFF) is a B cell–activating cytokine belonging to the TNF ligand family that has been associated with autoimmunity, but little is known about its effects on cancer immunity. We find that BAFF upregulates multiple B cell costimulatory molecules; augments IL-12a expression, consistent with Be-1 lineage commitment; and enhances B cell antigen-presentation to CD4+ Th cells in vitro. In a syngeneic mouse model of melanoma, BAFF upregulates B cell CD40 and PD-L1 expression; it also modulates T cell function through increased T cell activation and TH1 polarization, enhanced expression of the proinflammatory leukocyte trafficking chemokine CCR6, and promotion of a memory phenotype, leading to enhanced antitumor immunity. Similarly, adjuvant BAFF promotes a memory phenotype of T cells in vaccine-draining lymph nodes and augments the antitumor efficacy of whole cell vaccines. BAFF also has distinct immunoregulatory functions, promoting the expansion of CD4+Foxp3+ Tregs in the spleen and tumor microenvironment (TME). Human melanoma data from The Cancer Genome Atlas (TCGA) demonstrate that BAFF expression is positively associated with overall survival and a TH1/IFN-γ gene signature. These data support a potential role for BAFF signaling as a cancer immunotherapy.

Introduction

Immunotherapies that modulate T cell function have been firmly established as a pillar of cancer therapy, whereas the potential for B cells in the antitumor immune response is not well established. Beyond their well-defined role as antibody-producing cells, B cells contribute to immune regulation in a number of different ways. B cells are an important source of chemokines and cytokines and can modulate T cell responses to antigens (1, 2). B regulatory cells (Bregs) suppress T cell immunity through the secretion of IL-10 and TGF-β, whereas Be-1 effector B cells can augment Th1 responses through the secretion of cytokines, such as IL-12, and Be-2 effector B cells secrete cytokines classically associated with Th2 immune responses, including IL-4. Activated B cells also express high levels of MHC class II (MHCII) and serve as the predominant APCs to initiate CD4+ T cell responses under some physiological conditions (3–7). In addition to inducing Ag-specific T cell priming in vivo, B cells can express costimulatory signals required for CD4+ T cell clonal expansion and can break CD4+ T cell tolerance in vivo (4).

The importance of B cells in modulating T cell immunity is supported by the finding that B cell depletion may be an effective therapeutic strategy for certain autoimmune diseases for which T cells are the executioners of the immune response. For example, until very recently, pathogenic T cells were thought to be sufficient for the full manifestation of multiple sclerosis (MS); however, selective CD20+ B cell depletion has proven to be a highly effective treatment strategy for this autoimmune disease (8, 9). In addition to MS, B cell depletion has proven effective in other T cell–dependent autoimmune diseases, including rheumatoid arthritis and type 1 diabetes (10, 11). Since plasma cells, rather than CD20+ B cells, are the primary source of autoantibodies, and because the clinical benefits of B cell depletion on disease activity often precede any changes in autoantibody levels (12), this implies that B cells can modulate immunity independently of their modulation of autoantibodies in T cell–dependent diseases. While pathologic B cells have been implicated in the development of immune checkpoint toxicities, their role in modulating T cell immunity in cancer is

less established. Recent clinical efforts to break tolerance by depleting B cells have yielded mixed results in various preclinical models (13), likely because such efforts deplete both antitumor and immunoregulatory B cell subsets. The relevance of B cells in effective antitumor immunity is supported by recent studies in multiple tumor types, demonstrating that B cells in the TME before immune checkpoint inhibitor therapy are associated with enhanced responses to immune checkpoint blockade (14–16).

B cell–activating factor (BAFF), also known as B lymphocyte stimulator (BLyS) and TNF ligand superfamily member 13B (TNFSF13B), is a cytokine belonging to the TNF ligand family that activates B cells (17, 18). BAFF binds to 3 receptors that are primarily expressed on B cells: BAFF receptor (BAFF-R), B cell maturation antigen (BCMA), and transmembrane activator and CAML interactor (TACI). Prior studies have shown that a high number of autoreactive B cells enter into the periphery, but these autoreactive B cells are maintained in an anergic state, in part because they compete poorly for a limited supply of ambient BAFF (19). In this way, the scarcity of ambient BAFF may function as a B cell immune checkpoint. BAFF-Tg mice (20–22), as well as persons with a TNFSF13B gene polymorphism leading to increased soluble levels of BAFF (23), are at heightened risk of developing autoimmune disease; by contrast, BAFF-deficient mice have impaired B cell maturation and impaired T cell–dependent and T cell–independent immune responses (24, 25). The BAFF inhibitor belimumab was recently developed for the treatment of systemic lupus erythematosus (SLE). Whereas a link between BAFF and autoimmune disease is well established, little is known about how BAFF modulates cancer immunity. Here, we investigate the effect of BAFF on antitumor immunity and find that BAFF upregulates B cell costimulatory pathways, leading to downstream T cell activation and increased antitumor immunity.

Results

BAFF upregulates multiple B cell costimulatory molecules in vitro and induces a Be-1 phenotype in B cells. To characterize the effects of BAFF on B cells, we cultured isolated splenic B cells for 72 hours with or without recombinant BAFF and measured the expression of multiple cell surface markers by FACS. The addition of recombinant BAFF resulted in a marked increase in MHCII expression on B cells, as well as the T cell costimulatory markers CD40, CD80/86, and ICOS-L (Figure 1, A and B). BAFF also induced the expression of memory B cell markers (CD23 and CD21). Unexpectedly, BAFF induced high levels of expression of programmed death–ligand 1 (PD-L1) on B cells and a small but significant increase in CD5; both markers have been used in some contexts to identify Breg subsets. BAFF was also associated with an increase in B cell size, survival, and proliferation in vitro. In contrast to its marked effects on B cells in vitro, BAFF by itself did not demonstrate any effects on survival, memory, activation, or exhaustion of isolated CD4^{+} or CD8^{+} T cells in vitro (Figure 1, C–E).

To further elucidate the downstream effects of BAFF on B cells, we performed targeted gene expression analysis on isolated B cells cultured in vitro with or without BAFF for 48 hours. Consistent with our prior observations, the costimulatory markers ICOSL and CD40, as well as the MHCII-related genes H2-DMB2 and H2-Aa, were among the most differentially expressed genes (Figure 1F). BAFF also upregulated gene expression of IL-12a, a defining marker of Be-1 cells (1, 2) that is associated with Th1 priming and a Th1 immune response (Figure 1G). Gene expression of cytokines associated with Be-2 B cells (IL-2, IL-4, IL-6) or Bregs (IL-10 or TGF-β1) remained at low levels of expression with BAFF or were significantly decreased. Together, these findings indicate that BAFF may be involved in expansion or commitment of B cells to the Be-1 lineage, independently of antigen exposure or interactions with other cell subsets.

We also examined the effects of BAFF on multiple B cell surface markers and cytokines alone and in the context of B cell antigen engagement using a multiplex bead–based assay panel (Supplemental Figure 1; supplemental material available online with this article; https://doi.org/10.1172/jci.insight.136417DS1). B cell antigen engagement was simulated using an anti–mouse IgM antibody. Treatment with BAFF plus anti-IgM decreased PD-1 expression as compared with anti-IgM alone. While PD-1 can indicate either exhaustion or activation, other markers of B cell activation (CD69, MHCII, PD-L1, and CD40) were increased with BAFF alone and in combination with anti-IgM, supporting a role for BAFF in enhancing B cell activation and preventing B cell exhaustion in the context of B cell antigen engagement.

BAFF-activated B cells demonstrate enhanced antigen-presentation (APC) to CD4^{+} Th cells. Sufficient expression of MHC and costimulatory molecules are the defining characteristics of APC function, whereas upregulation of PD-L1 on APCs is associated with immune regulation through interactions with PD-1 and CD80. Since BAFF upregulated the expression of costimulatory markers (CD40, ICOSL, CD80/86) and MHCII
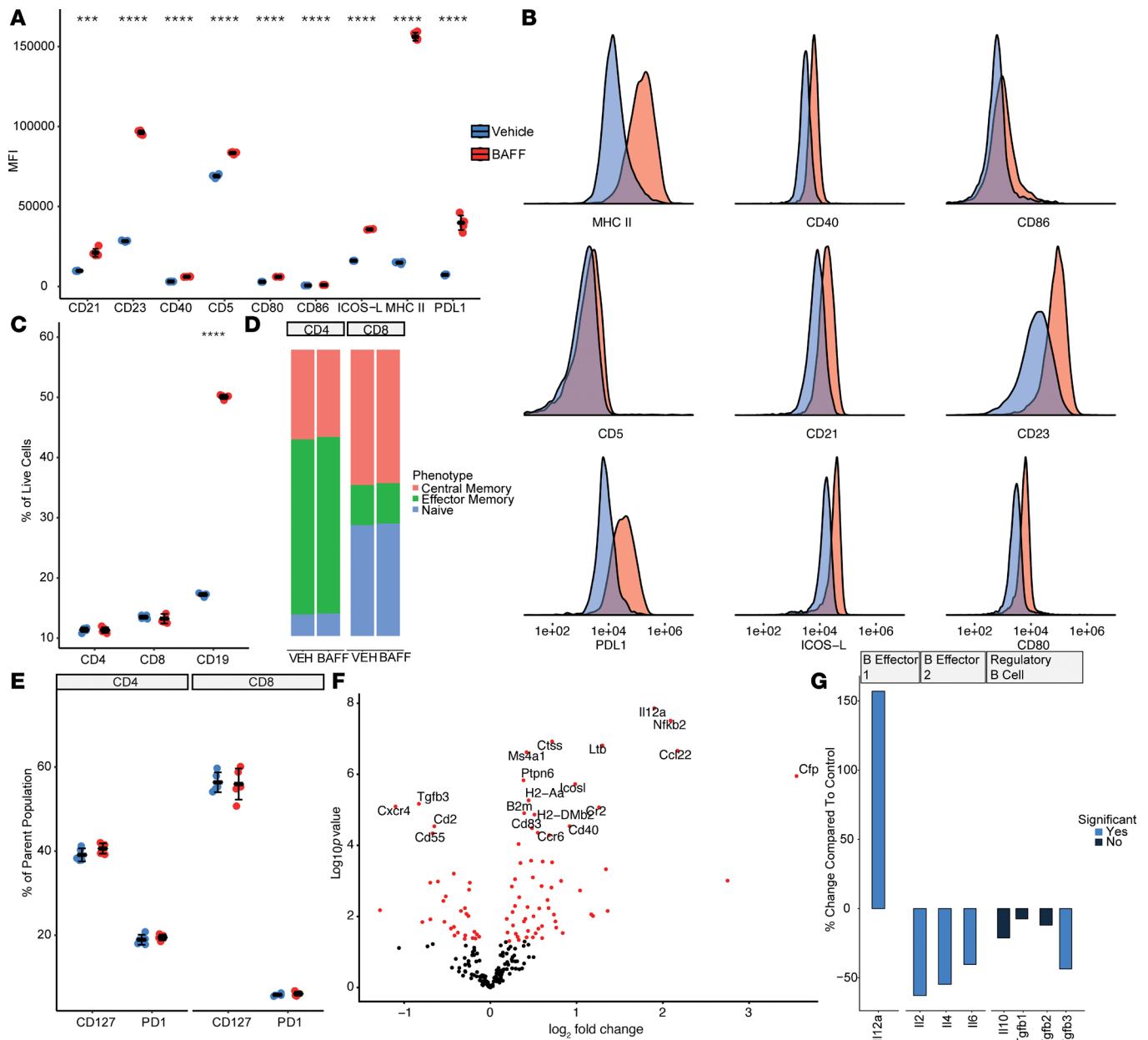
Figure 1. BAFF upregulates multiple B cell costimulatory molecules in vitro and induces a Be-1 phenotype in B cells. (**A**) Treatment of isolated B cells with BAFF in vitro significantly upregulates the expression of CD21, CD23, CD40, CD5, CD80, CD86, ICOS-L, MHCII, and PD-L1 ($n = 5$ per group, 2-tailed unpaired t test, ***$P < 0.001$, ****$P < 0.0001$) (**B**) Representative histograms describing the increase in MFI of B cell costimulatory molecules. (**C**) Treatment of whole splenocytes with recombinant BAFF in vitro increases the number of living B cells without significantly affecting T cells ($n = 5$ per group, 2-tailed unpaired t test, ***$P < 0.001$) (**D** and **E**) Similarly, in vitro treatment with BAFF does not change the phenotype or exhaustion profile of isolated T cells cultured with BAFF, suggesting that the downstream consequences of BAFF stimulation are most pronounced on B cells ($n = 5$ per group). (**F**) Targeted gene expression analysis of isolated B cells cultured with or without BAFF for 48 hours showed that the expression of ICOSL, CD40, H2-DMB2, and H2-Aa were among the most differentially expressed genes with BAFF ($n = 3$ per group). Significance was determined by nSolver's DE Call function and adjusted using the Benjamini-Yekutieli correction method. (**G**) BAFF leads to upregulation of IL-12a, suggesting enhanced B cell polarization toward a Be-1 phenotype, whereas expression of genes associated with a Be-2 or Breg phenotype were decreased with BAFF.

expression, but also upregulated the inhibitory ligand PD-L1, we investigated whether antigen presentation by BAFF-primed B cells to CD4+ T cells would be enhanced or inhibited. To address this question, we cultured isolated splenic B cells with and without recombinant BAFF for 24 hours, with a long OVA peptide (SLKISQAVHAAHAEINEAGR). The B cells were subsequently washed 3 times to remove excess BAFF and unbound OVA, and they were then cocultured with CD4+ T cells isolated from OT-II–Tg mice, which recognize the OVA peptide. B cells primed with BAFF were markedly more capable of activating CD4+ T
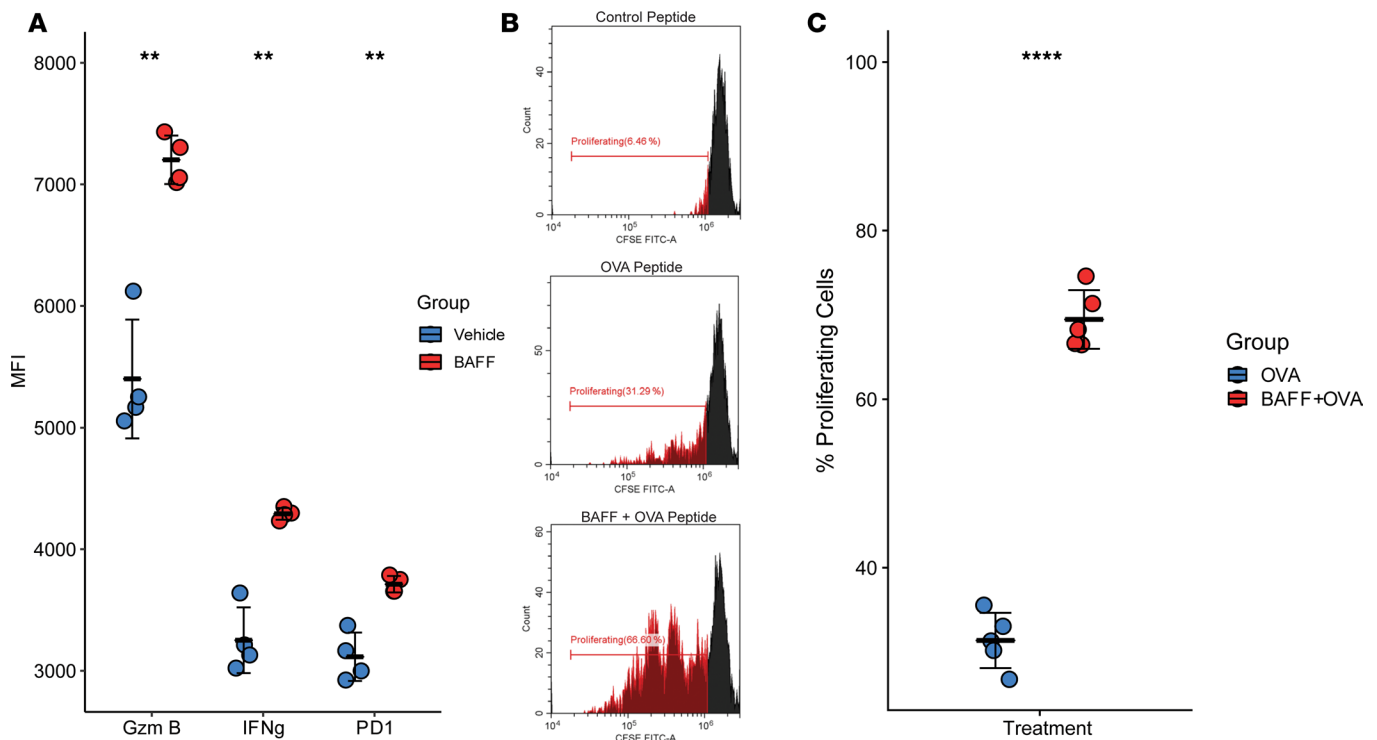
Figure 2. BAFF-activated B cells have enhanced antigen-presentation (APC) abilities for CD4⁺ Th cells. (**A**) CD4⁺ T cells from OT-II mice stimulated with B cells presenting SLKISQAVHAAHAEINEAGR peptides in the presence of BAFF expressed higher levels of granzyme B, IFN-γ, and PD-1. (**B** and **C**) Representative histograms and summative graph demonstrating the increased ability of BAFF-activated B cells to present antigens and stimulate OT-II CD4⁺ T cell proliferation. The Rpo132 peptide is used as the negative control (n = 5 per group, **$P < 0.01$, ****$P < 0.0001$, 2-tailed unpaired t test).

cells from an OT-II–Tg mouse as compared with B cells that were not primed with BAFF, indicated by increased expression of intracellular cytokines IFN-γ and granzyme B (GNZb), as well as PD-1, on CD4⁺ T cells (Figure 2A). Furthermore, B cells primed with BAFF markedly increased proliferation of CD4⁺ T cells from an OT-II mouse in the presence of OVA-albumin ligand, as compared with B cells that were not primed with BAFF (Figure 2, B and C). BAFF-primed B cells cultured with a control peptide (AVNIHVLTTPGL-NHAFSSLL, a multisubunit RNA polymerase encoded by vaccinia virus) and cocultured with CD4⁺ T cells from an OT-II–Tg mouse did not elicit T cell activation or expansion (data not shown), indicating that the CD4 response was antigen specific. BAFF did not improve the ability for B cells to cross-present to CD8⁺ T cells isolated from an OT-I mouse (Supplemental Figure 2). The B cells used as professional antigen-presenting cells (APCs) in this assay are not specific for the OVA peptide and, therefore, indicate a potential role for BAFF in enhancing presentation of nonspecific antigens to CD4⁺ T cells. However an important mechanism through which B cells present to CD4⁺ T cells in vivo is through high-efficiency presentation of specific antigens mediated through the B cell antigen receptor. We therefore investigated the effect of BAFF in an in vivo tumor model via which presentation of specific antigen through the B cell antigen is anticipated to occur.

BAFF augments Th1 responses within the TME and promotes antitumor immunity in vivo, but also has distinct immunoregulatory functions. After determining that BAFF activates multiple B cell costimulatory molecules, upregulates B cell IL-12a expression consistent with Be-1 lineage commitment, and enhances APC abilities for CD4⁺ Th cells in vitro, we hypothesized that BAFF may augment antitumor T cell immunity in vivo. To determine the effects of BAFF on immune populations in a tumor-bearing in vivo model, C57BL/6J mice were challenged with 1×10^4 B16F10 tumor cells orthotopically implanted into the right flank, followed by treatment with recombinant BAFF (0.5 mg/kg) or vehicle administered daily beginning on day 7. On day 14, when tumors were approximately 7 × 7 mm, we performed an in-depth analysis of T and B cell subtypes and their functional status.

BAFF and vehicle-treated spleens were analyzed with multipanel mass cytometry, cytometry by TOF (CyTOF), using unsupervised clustering and hierarchal gating analysis of the debarcoded CyTOF data sets (Figure 3, A–I). We found that, in the spleen, recombinant BAFF primarily modulates the B cell compart-
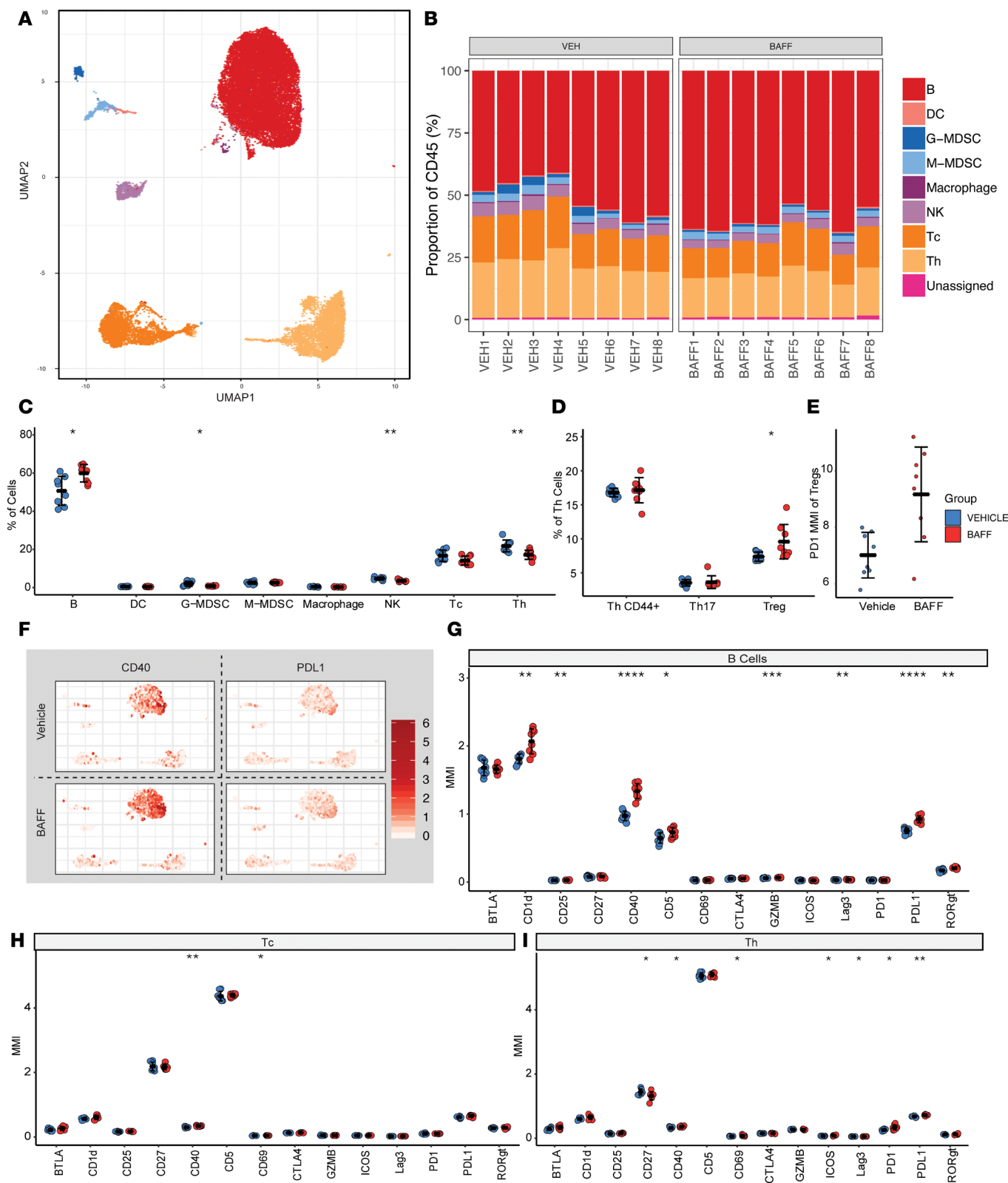
Figure 3. BAFF augments Th1 responses and promotes antitumor immunity, but also has distinct immunoregulatory functions. (A) Uniform manifold approximation plot (UMAP), a dimensionality reduction technique to visualize similar cell proteomic characteristics in 2 dimensions, shows clustering results of 16 spleen samples (8 biological replicates for each of the 2 experimental arms) analyzed by mass cytometry. A total of 2000 events per sample is shown. Each color represents a specific immune cell type, as annotated based on marker intensity profiles. Color legend is shown with B. (B) Immune cell composition within each of the spleen samples are shown in stacked bar graphs as a percentage of CD45$^+$ cells. (C) BAFF treatment increases the proportion of B cells in the spleen, while decreasing G-MDSC, NK, and Th cell populations. (D) Of the Th cell fraction, BAFF treatment increases the proportion of CD44$^+$ cells, while decreasing the proportion of Tregs. (E) BAFF treatment increases the mean signal intensity of PD-1 in Tregs taken from the spleen.

(**F**) Mass intensity heatmaps for each of the 2 immune markers, CD40 and PD-L1, are superimposed onto the UMAP representation of the cell clusters, as shown in **A** for the 2 experimental groups, vehicle- and BAFF-treated. (**G**) BAFF treatment affects B cells by increasing the proportion of B cells expressing CD1d, CD25, CD40, CD5, GZMB, Lag3, PD-L1, and RORγt (statistically significant changes). (**H**) BAFF treatment affects CD8$^+$ cytotoxic T (Tc) cells by increasing the proportion of Tc cells expressing CD40 and CD69. (**I**) BAFF treatment affects Th cells by increasing the proportion of Th cells expressing CD40, CD69, ICOS, Lag3, PD-1, and PD-L1, while decreasing the proportion of cells expressing CD27. Two-tailed unpaired t tests were used to compare vehicle and BAFF groups; *$P < 0.05$, **$P < 0.01$, ***$P < 0.001$, ****$P < 0.0001$.

ment, with more subtle changes to other lymphocyte compartments. The total percentage of splenic B cells was increased with concomitant decreases in percentages of other immune cell compartments (Figure 3, B and C). Within the Th cell compartment, there was a statistically significant increase in the number of FoxP3$^+$ Tregs. These Tregs also had increased expression of PD-1 (Figure 3D). Within the B cell compartment, expression of CD40 and PD-L1 was increased (Figure 3G), consistent with the effects of BAFF in vitro. BAFF also increased expression of CD1d, CD25, CD5, GNZMB, Lag3, and RORγt on splenic B cells, and it increased activation of innate immune populations within the spleen (Supplemental Figure 3). Within the T cell compartment, BAFF treatment was associated with increased activation of both cytotoxic and Th cells, as indicated by increased CD69 expression (Figure 3, H and I). In addition, CD40 expression was increased in T cells, which is a costimulatory molecule for T lymphocytes, and the inducible costimulator ICOS was induced on Th cells. Notably, CD27 was significantly decreased in Th cells, which marks an activated population of induced effector memory cells (26). Together, these results indicate that, while BAFF predominantly activates and expands splenic B cell populations, T cell activation and maturation is a downstream consequence of BAFF therapy. These results also indicate that these changes occur in association with an increase in splenic FoxP3$^+$ Tregs.

We subsequently looked at changes within the tumor draining lymph node and TME by FACS with recombinant BAFF treatment (Figure 4, A–D). Similar to what was observed in the spleen, BAFF treatment was associated with an increase in B cells and a decrease in T cell subsets as a percentage of total CD45 events in the tumor draining lymph node. A higher percentage of both CD8$^+$ and CD4$^+$ T cells within the tumor draining lymph node were of a central memory phenotype (CD62L$^+$, CD44$^+$), whereas naive T cells (CD62L$^+$, CD44$^-$) were decreased. CCR6 expression was significantly increased in CD4$^+$ T cells in tumor draining lymph nodes, and this receptor is thought to play a role in the recruitment of inflammatory T cells as well as Tregs to certain inflammatory sites, particularly in autoimmune diseases (27).

Within the TME, BAFF treatment was associated with enhanced activation and a Th1-associated inflammatory response (Figure 4, A–G). Isolated T cells from within the TME demonstrated an increase in TH1 CD4$^+$ T cells, as well as T-bet$^+$CD8$^+$ T cells. Gene expression analysis of isolated CD45$^+$ immune cells from a tumor further demonstrated that BTLA and CD69 were 2 of the most positively differentially expressed genes with BAFF. BTLA is an inhibitory ligand preferentially expressed by Th1 but not Th2 cells, and CD69 is an early marker of activation, consistent with an exaggerated Th1 response. Concomitantly, BAFF treatment was associated with an increase in FOXP3$^+$CD4$^+$ Tregs within the TME, and this increase characteristically impedes effective antitumor immunity. Although total numbers of Tregs were increased with BAFF treatment, there was also increased expression of IFN-γ within these intratumoral Tregs (IFN-γ$^+$ Tregs). Expression of IFN-γ on Tregs is thought to identify a population of "fragile" Tregs with loss of suppressive activity (28).

The data indicate that systemic BAFF has intricate effects on antitumor immunity, increasing T cell activation and exaggerating TH1 responses, but also increasing the total number of Tregs. However, a subset of these intratumoral Tregs are converted a "fragile" Treg phenotype. To determine whether these immune changes resulting from BAFF treatment had a perceptible effect on tumor growth dynamics, we extended treatment with BAFF and followed tumors for survival (Figure 4F). BAFF was consistently associated with a significant delay in tumor growth in the B16F10 melanoma model ($P < 0.01$). Thus BAFF had an overall positive effect on antitumor immunity in the B16F10 melanoma model.

BAFF is an effective adjuvant for therapeutic anticancer vaccines. Systemic administration of BAFF for therapeutic purposes may be challenging, due to expression of BAFF-R on a wide range of different cell types (29) and theoretical concerns about autoimmunity. Therefore, we also evaluated the potential for BAFF as an adjuvant for therapeutic cancer vaccines, which could mitigate the potential for off-target effects of systemic BAFF. We hypothesized that the enhancement of B cell activation in vaccine-draining lymph nodes, and increased expression of B cell costimulatory molecules and antigen presentation, would enhance T cell activation and antitumor immunity. To test this hypothesis, we created a nontumorigenic murine cell line that constitutively secreted high levels of soluble mouse BAFF (3T3-BAFF). We subsequently investigated
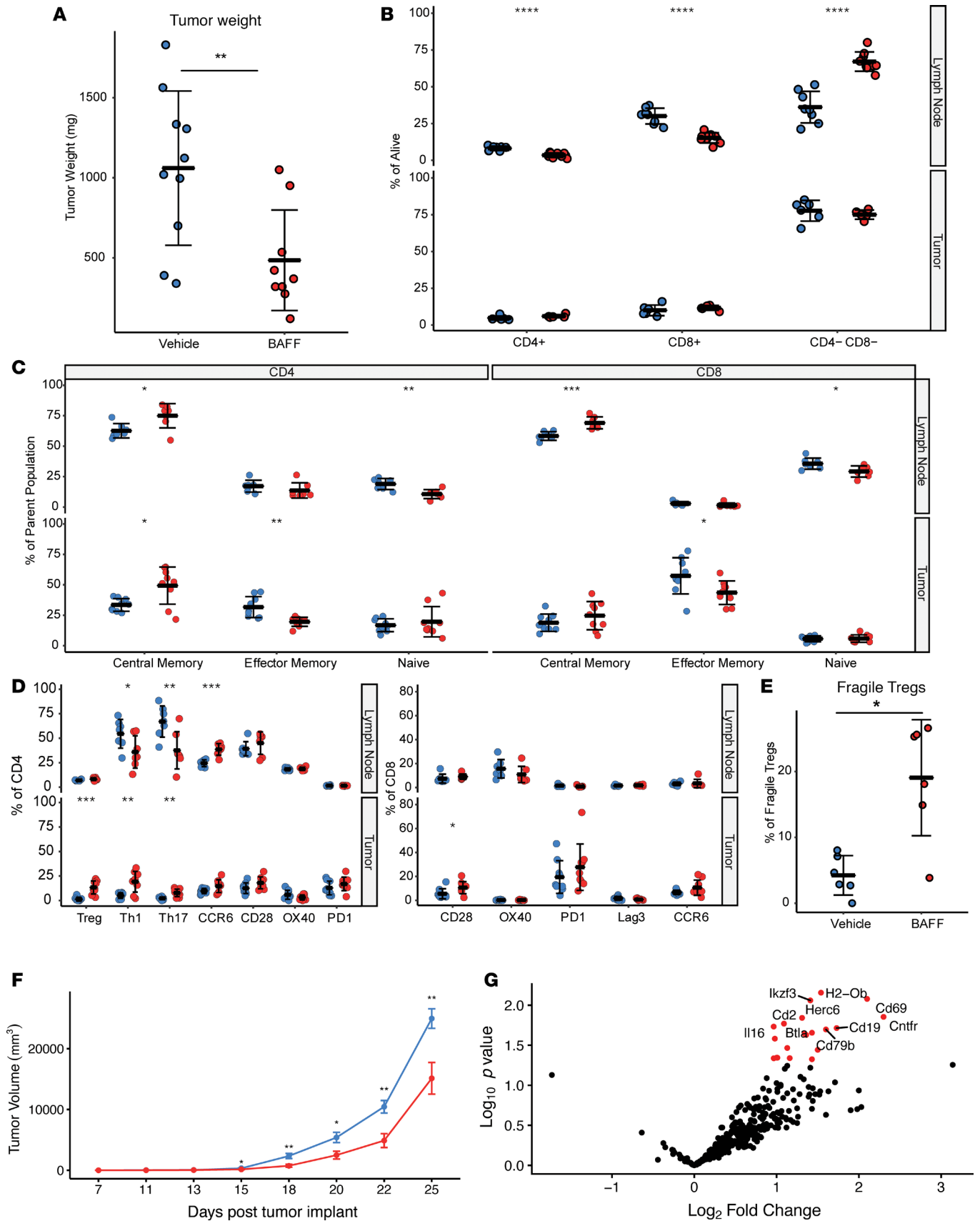
Figure 4. BAFF increases T cell activation in vivo but also induces an increase in Treg frequency. C57BL/6J mice were challenged with B16F10, followed by treatment with recombinant BAFF (0.5 mg/kg) or vehicle (n = 10 per group) daily beginning on day 7 after tumor implantation. (**A**) Tumor weights at the time of resection demonstrated significantly decreased tumor weights in the BAFF treatment group. (**B**) BAFF increases the proportion of B cells and decreases the proportion of CD4$^+$ and CD8$^+$ T cells within the lymph node. (**C**) BAFF treatment increases central memory cells and decreases naive T cells in the lymph node and TME. (**D**) BAFF treatment markedly enhances the proportion of CCR6-expressing CD4$^+$ T cells in tumor draining lymph nodes. Expression of CCR6 on CD4$^+$ T cells in lymph nodes parallels an increase in the proportion of Treg, Th1, and Th17 CD4$^+$ T cells within the TME. (**E**) Treatment of BAFF was associated with the upregulation of IFN-γ$^+$ within a subset of Tregs in the TME, consistent with a "fragile" Treg phenotype. (**F**) In vivo treatment of B16F10 tumors with recombinant BAFF significantly delays tumor growth. Tumor growth curves for vehicle (blue) and BAFF (red). Mean ± SEM, n = 12 per group. (**G**) Volcano plot showing significantly upregulated genes in BAFF-treated TIL. n = 3 per group; significance was determined by nSolver's DE Call function and adjusted using the Benjamini-Yekutieli correction method. Two-tailed unpaired t test were used to compare vehicle and BAFF group weights and cell phenotypes; *$P < 0.05$, **$P < 0.01$, ***$P < 0.001$, ****$P < 0.0001$.

the utility of BAFF as a vaccine adjuvant, using the 3T3-BAFF cell line as a bystander BAFF-secreting vaccine in combination with irradiated autologous tumor cells. The 3T3-BAFF vaccine (3×10^6 irradiated 3T3-BAFF cells plus 3×10^6 irradiated B16F10 cells) was injected s.c. in 3 limbs, and tumor draining lymph nodes were collected 7 days after treatment. A 3T3-Mock vaccine (3×10^6 irradiated 3T3-Mock cells plus 3×10^6 irradiated B16F10 cells) was used as a negative control.

Similar to our findings in tumor-draining lymph nodes with systemic BAFF, we found that the 3T3-BAFF vaccine resulted in an increase in CD19$^+$ B cells and a relative decrease in CD4$^+$ and CD8$^+$ T cells, as a percentage of total events compared with the 3T3-Mock vaccine (Figure 5, A–C). The absolute number of T cells was unchanged between the 3T3-BAFF and 3T3-Mock vaccine draining nodes, indicating that BAFF increased the number of B cells rather than decreased the number of T cells in these nodes. The B cells within the vaccine draining nodes also expressed increased CD40 and PD-L1, consistent with the previously observed effects of BAFF in vitro. Within the T cell compartment, the proportion of both CD4$^+$ and CD8$^+$ T cells with central memory markers (CD62L$^+$CD44$^+$) was increased and paralleled a decrease in the number of naive T cells, consistent with increased antigen presentation within the lymph node. We subsequently investigated whether BAFF could augment the antitumor immunity of whole cell vaccines by vaccinating with irradiated 3T3-BAFF or 3T3-Mock cells plus irradiated allogeneic tumor cells on day 3 after tumor implantation. Using multiple allogeneic tumor models, we found that BAFF as a vaccine adjuvant consistently showed a positive trend or significantly delayed tumor growth (Figure 5, D–G), which was dependent on the presence of B cells (Supplemental Figure 4). Therefore, similar to the effects of systemic BAFF, the use of BAFF as a vaccine adjuvant had a positive effect on antitumor immunity.

BAFF expression is associated with a TH1 gene signature and improved survival in human melanoma. After identifying that BAFF augmented antitumor immunity in a preclinical models of melanoma, we attempted to extend our findings to human cancers using metastatic melanoma data from The Cancer Genome Atlas (TCGA). We examined whether BAFF expression within the tumor microenvironment was correlated with patient survival. Since BAFF expression is a continuous variable, we examined different cutoffs for BAFF expression including 50th percentile and 90th percentile. Using various cutoffs, a higher BAFF expression level was consistently associated with improved 5-year overall survival (OS) (BAFF cutoff 0.5, $P < 0.001$, hazard ratio for survival [HR] = 0.53; BAFF cutoff 0.9 $P = 0.004$, HR = 0.37) (Figure 6, A–C). We also examined the relationship between BAFF expression and genes associated with a Th1 gene signature. Consistent with our preclinical findings, we found that expression of BAFF was strongly associated with multiple molecules that are characteristic of Th1 signaling, including STAT1 and IFN-γ (Figure 6D).

Discussion

In summary, we find that BAFF has distinct effects on B and T cells that contribute to antitumor immunity (Figure 7). Specifically, BAFF activates B cells expressing high levels of costimulatory molecules (CD40, ICOSL), augments antigen presentation to CD4$^+$ T cells through increased expression of MHCII, and increases IL-12 expression to promote the differentiation of TH1 cells and T cell memory. Our findings identify the BAFF signaling pathway as a potential costimulatory pathway that can augment antitumor immunity. Unlike other costimulatory molecules in development (including but not limited to CD137, CD27, and ICOS), the BAFF signaling axis is unique because it predominantly activates B cells (30). While a beneficial role for B cells in the antitumor immune response is less established than that of T cells, our results add to an emerging body of literature demonstrating the potential for B cell activation in enhancing T cell responses and improving outcomes during cancer immunotherapy (14–16, 31, 32).
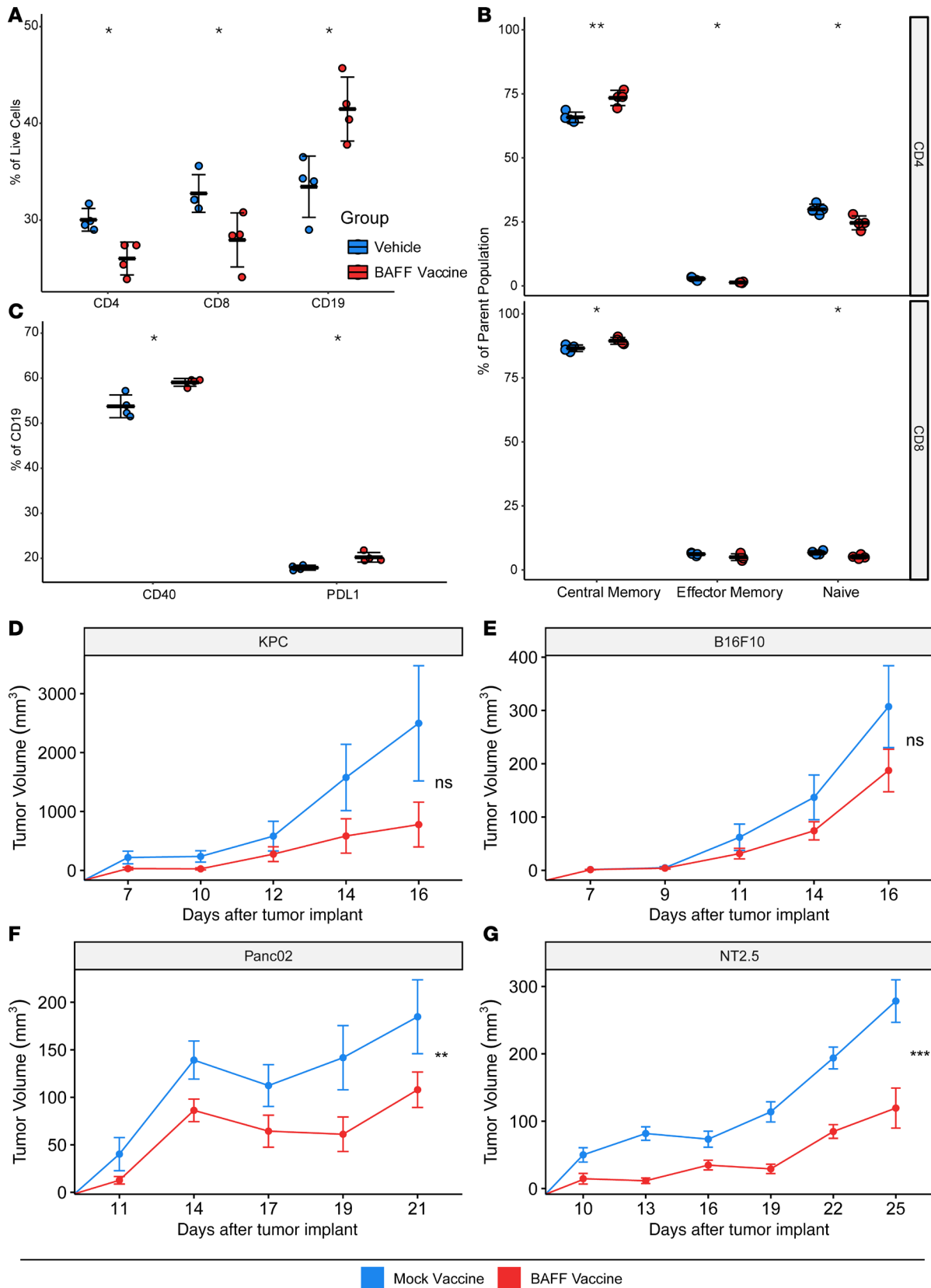
Figure 5. BAFF treatment is an effective cellular adjuvant for anticancer vaccines. (**A**) BAFF vaccine treatment reduces the proportion of CD4+ and CD8+ T cells while increasing the proportion of B cells in vivo. $n = 4$. (**B**) BAFF vaccine treatment supports the central memory phenotype of both CD4+ and CD8+ T cells in vivo. $n = 4$. (**C**) BAFF vaccine treatment increases the proportion of B cells expressing CD40 and the proportion of B cells expressing PD-L1. $n = 4$. (**D–G**) BAFF vaccine treatment delays the tumor progression of KPC, B16F10, Panc02, and NT2.5 tumor models. Results are shown as mean ± SEM ($n = 10$ per arm), 2-tailed unpaired t tests. *$P < 0.05$, **$P < 0.01$, ***$P < 0.001$.
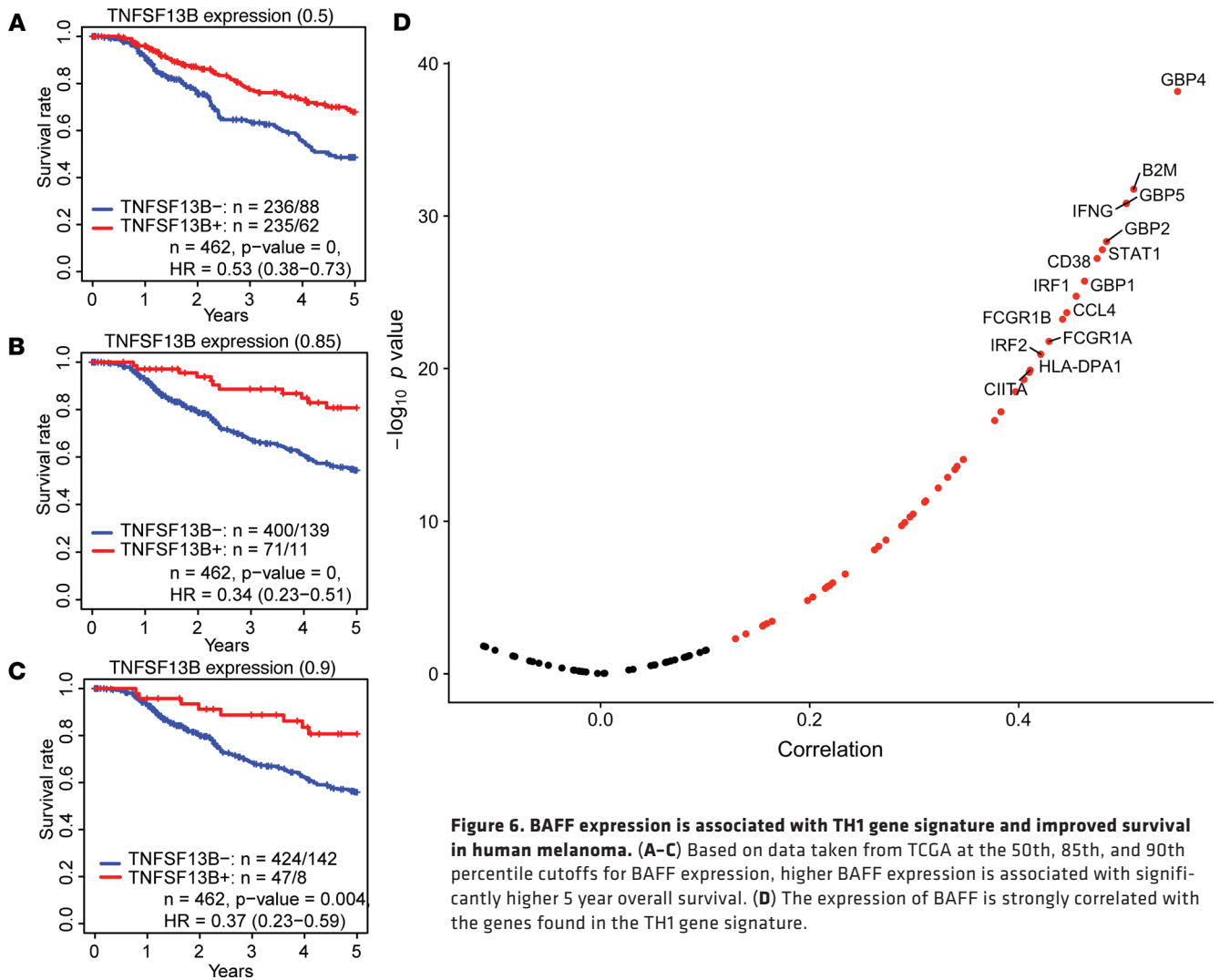
Figure 6. BAFF expression is associated with TH1 gene signature and improved survival in human melanoma. (A–C) Based on data taken from TCGA at the 50th, 85th, and 90th percentile cutoffs for BAFF expression, higher BAFF expression is associated with significantly higher 5 year overall survival. **(D)** The expression of BAFF is strongly correlated with the genes found in the TH1 gene signature.

Our findings build upon the work of other groups that have investigated the effects of BAFF on other disease processes using BAFF-Tg mouse models. These prior studies have demonstrated a complex role for BAFF immunomodulation. Similar to its described effects within the tumor microenvironment, BAFF has previously been shown to augment certain Th1-associated inflammatory responses and to suppress Th2-associated responses (33). Our findings also provide context for the counterintuitive observation that BAFF-Tg mice, despite displaying features of autoimmunity, are also immunocompromised, as indicated by their acceptance of islet allografts and delayed skin graft rejection (34), and for the finding that blocking BAFF signaling in MS (an autoimmune disease associated with high systemic BAFF levels) may paradoxically increase disease activity (35). After 7 days of recombinant BAFF treatment in our tumor model, we did observe an increase in B cell suppressive markers (PD-L1, CD5, and CD1d), as well as an increase in CD4+Foxp3+ Tregs. We hypothesize that the observed increase in Tregs may be related to enhanced antigen presentation of nonspecific antigens, including self-antigens. Prior studies have shown an important role for B cells in inducing Treg differentiation and expansion for T cells that recognize nonspecific antigenic epitopes presented by B cells (36), and our in vitro model suggests that nonspecific antigen presentation is markedly enhanced by BAFF. We hypothesize that, in BAFF-Tg mice, chronic B cell nonspecific presentation of self-antigens, as well as chronic costimulation of T cells, leads to a compensatory reestablishment of tolerance and chronically suppressed T cell effector responses. The observed immunoregulatory changes associated with BAFF treatment were insufficient to suppress antitumor activity. The enhanced antitumor activity observed with BAFF may be due in part to the conversion of intratumoral Tregs to a less suppressive "fragile" phenotype (28). The observation of increased PD-L1 expression on B cells in the context of BAFF
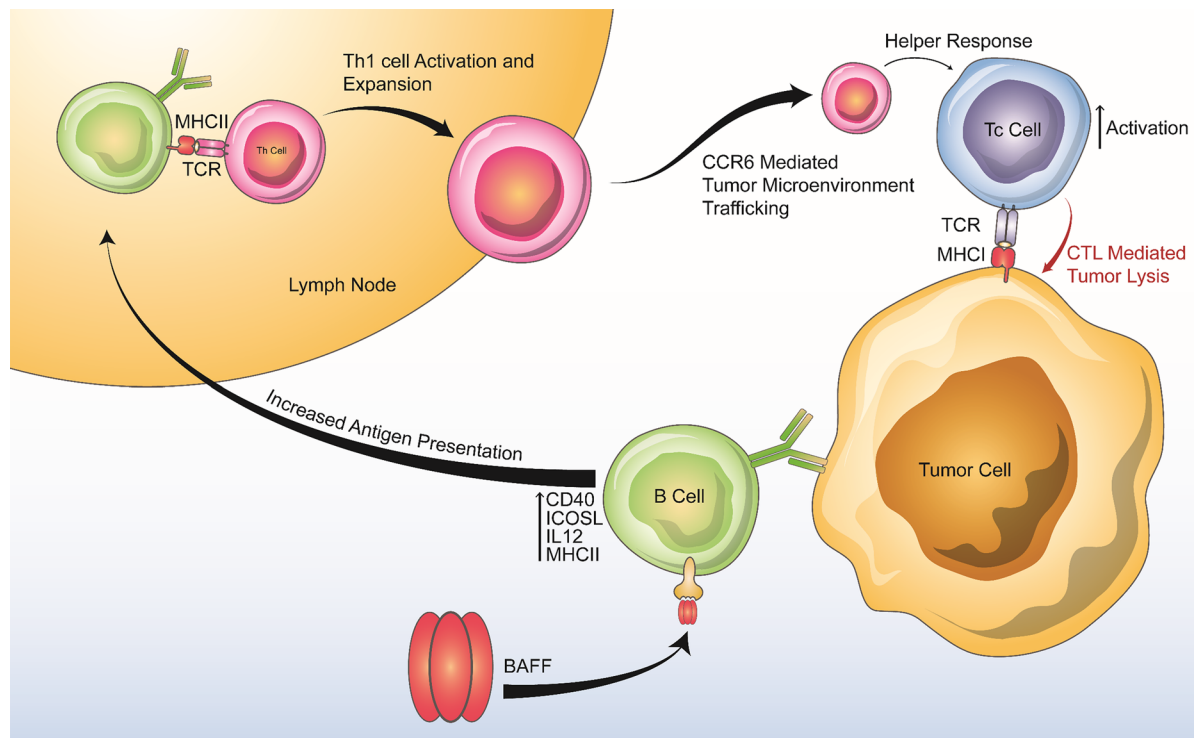
Figure 7. Summary of BAFF's positive effects on anti-tumor immunity. BAFF increases B cell antigen presenting activity, production of Th1 cytokines, and costimulatory molecule expression, leading to downstream Th1 activation and expansion, enhanced chemotaxis of proinflammatory cells via the CCR6-CCL20 axis, and enhanced Tc-mediated tumor lysis.

provides initial evidence that the antitumor activity of BAFF may be augmented by inhibitors of the PD-1/PD-L1 axis, and investigation of BAFF in combination with immune checkpoint therapy is warranted.

Whether systemic administration of BAFF is feasible remains unclear, given theoretical concerns about off-target direct effects of BAFF on malignant cells (29), as well as the potential for autoimmune side effects. Encouragingly, we did not observe any adverse events related to BAFF in any of our experimental preclinical conditions. Furthermore, a phase 1 dose escalation study of systemic BAFF was previously conducted in at the National Cancer Institute (NCI) for the treatment of IgA deficiency (NCT00024934; https://clinicaltrials.gov/ct2/show/NCT00024934), and although BAFF was not effective for this indication, the preclinical and clinical studies associated with this effort supported the safety of systemic BAFF (Warren Strober [National Institute of Allergy and Infectious Diseases, Bethesda, MD, USA], personal communication). The use of BAFF as a vaccine adjuvant could partially mitigate toxicity concerns by limiting systemic BAFF exposure. Our observation that BAFF may augment therapeutic vaccine responses in whole cell cancer vaccines builds upon the work of Shurin and colleagues, who find that BAFF is vital for the antitumor activity of dendritic vaccines (37). Additionally, BAFF has been previously shown to augment vaccine responses against a number of bacterial and viral antigens (38–42).

BAFF binds to 3 known receptors (BAFF-R, BCMA, and TACI); therefore, it is unclear which downstream receptors are responsible for augmenting antitumor immunity and whether the BAFF axis may be more specifically targeted through agonism of a specific BAFF-R. The BAFF-R costimulatory receptor is widely expressed on circulating lymphocytes and is the most likely candidate for augmenting antitumor responses, whereas BCMA has limited expression and is believed to primarily enhance plasma cell survival in BM (17, 43). BAFF signaling via the TACI receptor has complex effects on multiple immune subsets but may act as a compensatory immunosuppressive pathway to maintain immunological homeostasis in the setting of elevated BAFF. TACI signaling can decrease B cell activation in some contexts and can promote expression of Foxp3, IL-10, and PD-L1 in Tregs (44–46). Therefore, it is possible that the observed antitumor effects of systemic BAFF could be improved by specifically targeting the BAFF-R, while avoiding the inhibitory effects of TACI signaling. Additional research is needed to understand the

specific contributions of each of the BAFF-R on antitumor immunity. In conclusion, the BAFF signaling axis may augment antitumor immune responses, and additional investigation of BAFF signaling in the context of tumor immunity is warranted.

Methods

Recombinant BAFF. All recombinant BAFF experiments used a single batch of recombinant mouse BAFF purchased in bulk from R&D systems (catalog 8876-BF-010, bottled on 10/23/2018). The BAFF was produced in a mouse myeloma cell line (NS0), was > 85% pure by SDS-PAGE, and had low endotoxin level (<0.01 EU per 1 μg of protein by the limulus amebocyte lysate [LAL] method). Preliminary experiments by our group confirmed the effects of recombinant BAFF on B cells in vitro using recombinant mouse BAFF protein from a different vendor (Abcam, catalog ab157285) and using a different batch of recombinant mouse BAFF from the same vendor (R&D systems), without perceptible batch effects.

In vitro experiments. Splenocytes were pooled from 2 mature C57BL/6J mice purchased from the Jackson Laboratory, and B cells were isolated using a using a negative selection method (EasySep Mouse B Cell Isolation Kit, Stemcell Technologies, catalog 19854) following the manufacturer protocol. B cell purity of > 99% was confirmed after isolation by FACS. The isolated B cells were subsequently cultured in a 48-well plate at a density of 1 million cells/mL in 300 μL of CTL media (RPMI [Thermo Fisher Scientific], 10% FBS [BenchMark], 2-mercaptoethanol 0.1% [Thermo Fisher Scientific]) with or without 5 μg/mL of recombinant BAFF (mouse BAFF protein, R&D Systems) or 0.5 mg/mL goat anti–mouse IgM (catalog 1021–01, SouthernBiotech) for 72 hours at 37°C. After washing, samples were transferred to a 96-well plate and stained for FACS. Determination of the effects of recombinant BAFF on isolated CD4$^+$ and CD8$^+$ T cells was performed in parallel using the EasySep Mouse CD4 and CD8 Cell Isolation Kits, respectively

To determine the effect of BAFF on gene expression within B cells, we isolated B cells from the spleens of 2 mature C57BL/6J mice, using a negative selection method as described above. Isolated B cells were subsequently cultured in a 48-well plate at a density of 1 million cells/mL in 300 μL of CTL media (RPMI, 10% FBS, 2-mercaptoethanol 0.1%) with or without 5 μg/mL of recombinant BAFF (mouse BAFF protein, R&D Systems) for 48 hours at 37°C. Cells were washed 3 times in PBS and pooled into 6 wells (3 BAFF-treated, 3 vehicle treated) for RNA extraction. RNA was isolated using a Zymo Direct-zol RNA kit following the manufacturer protocol. RNA was quantified on Thermo Fisher NanoDrop 2000 and measuring using NanoString nCounter Immunology Panel (Mouse). Data were analyzed on Nanostring nSolver.

We next studied the effectiveness of BAFF-expanded B cells in presenting antigen and coactivating T cells in vitro. We isolated 5×10^5 B cells from a mature C57BL/6J mouse using a negative selection method (EasySep Mouse B Cell Isolation Kit, Stemcell Technologies) as described above. These isolated B cells were cultured in 300 μL of CTL media for 24 hours in the presence of 2 ng/μL of OVA OT1 peptide (GLE-QLESIINFEKLTEWTSS) or OTII peptide (SLKISQAVHAAHAEINEAGR), with or without 5 μg/mL of recombinant BAFF. Separately, isolated B cells were cultured with vehicle or a control peptide (Rpo132, AVNIHVLTTPGLNHAFSSLL; Ttn, IKIVRLTTGSAYQFRVCAEN; Pnpla7, LSGWWLLWKRCN-PLATKVKV) as negative controls. The B cells were subsequently spun and washed in PBS 3 times to ensure that unbound BAFF and peptide were removed, and only peptide processed by the B cells remained. The B cells were subsequently cocultured in 1 mL of CTL media for 72 hours, with 1×10^6 CD4 T cells (EasySep Mouse CD4$^+$ T Cell Isolation Kit, Stemcell Technologies) isolated from a B6.Cg-Tg(TcraTcrb)425Cbn/J (OT-II) mouse spleen, purchased from the Jackson Laboratory. OTII mice express a mouse α-chain and β-chain T cell receptor that pairs with the CD4 coreceptor and is specific for OVA in the context of MHCII. After 72 hours of coculturing, the cells were spun, washed 3 times in PBS, and then stained for FACS. These experiments were repeated with CFSE labeling of T cells before coculturing, following the manufacturer staining protocol (CellTrace CFSE Cell Proliferation Kit).

Recombinant BAFF in vivo experiments. C57BL/6J mice were purchased from the Jackson Laboratory and allowed to acclimate for at least 1 week before experiments. The B16F10 cell line was purchased from ATCC. B16F10 cells were cultured in DMEM media supplemented with 10% FBS (Gemini), 1% L-glutamine (Invitrogen), and 0.5% penicillin/streptomycin (Invitrogen). Cells were cultured for a week before implantation, and passage numbers 3–5 were used.

C57BL/6J mice were challenged s.c. with 5×10^4 tumor cells in the hind leg, followed by treatment 7 days later. BAFF (0.5 mg/kg) was administered daily for 7 days i.p. Mice were sacrificed and tissues were collected 14 days after tumor implantation. Tumors were cut into small chunks and processed on a

gentleMACS Octo Dissociator (Miltenyi Biotec)using the manufacturer soft tumor program. Following dissociation, tumors were quenched with 5 mL of DMEM complete media and passed through 100-mm cell strainers (Falcon) to further break up any bound tumor cells. One additional 5-mL wash was performed on the C-tube and passed through the cell strainer. A final 5-mL wash on the cell strainer was preformed to flush the strainer. The flow through was spun and ACK lysis was performed. A total of 1×10^6 cells was plated in a 96-well plate for FACS (Quality Biological, catalog 118-156-721).

For gene expression analysis, after dissociation, the flow through was purified on Miltenyi autoMACS using CD45$^-$ isolation. Total CD45 isolated cells were placed into Trizol LS and stored at –80°C. Samples were thawed to room temperature and processed using Zymo Direct-zol RNA kit. RNA was quantified on Thermo Fisher NanoDrop 2000, and isolated RNA was stored at –80°C. NanoString immunology 360 panel was run on samples in triplicate (vehicle and BAFF) at 100 ng/per sample concentration. Data were analyzed using NanoString nSolver and graphed using R-studio.

For survival studies, C57BL/6J mice were challenged s.c. with 1×10^4 tumor cells in the hind leg, followed by treatment 7 days later. BAFF (0.5 mg/kg) was administered 3 times weekly i.p. Tumor length and width were assessed at least 3 times weekly using caliper measurements, with the length assigned to the longest cross-sectional tumor diameter. Tumor volume was calculated as (tumor volume = [length × width^2]/2). Tumor volume was assessed until tumors reached 20 × 20 mm, at which point the mice were euthanized.

FACS staining and analysis. Isolated single cell suspensions were washed and then incubated for 30 minutes with Live/Dead Near-IR (Thermo Fisher Scientific, catalog L10119) according to the manufacturer's protocol, followed by a 30-minute incubation with the appropriate flow cytometry antibodies. For samples being analyzed for cytokine expression, a protein transport inhibitor cocktail (eBioscience, catalog 00-4980-03) was introduced during the last 4–6 hours of stimulation according to the manufacturer protocol. Samples stained for intracellular markers were fixed and permeabilized before intracellular staining using a transcription Factor Fixation/Permeabilization kit (eBioscience, catalog 00-5523-00). A list of antibodies and concentrations used is listed in Supplemental Table 1. All samples were run on a Beckman Coulter Cytoflex. Data were analyzed with FlowJo v10.5 (TreeStar Inc.).

LegendPlex bead–based assay for cytokine analysis. B cells were treated with 5 μg/mL of recombinant BAFF (mouse BAFF protein, R&D Systems) or with 0.5 mg/mL of goat anti–mouse IgM (catalog 1021–01, SouthernBiotech) or BAFF$^+$ anti-IgM combination treatment in 500 μL of CTL media. Supernatant was removed from each well after 72 hours and was processed using the LEGENDplex Mouse B cell Panel (BioLegend, catalog 740818) according to the manufacturer's protocols. All samples were run on a Beckman Coulter Cytoflex. Data were analyzed with LEGENDplex Data Analysis Software v8.

CyTOF data acquisition and analysis. A list of mass cytometry antibodies, isotopes, and concentrations used for immune profiling the spleen samples is shown in Supplemental Table 2. Conjugation of primary antibodies was performed using Maxpar Conjugation Kits (Fluidigm) according to the manufacturer's protocol. Briefly, purified antibodies were run through a buffer exchange protocol using 50 kDa ultra filtration columns (Amicon) and then partially reduced with 4 mM TCEP (Thermo Fisher Scientific). Polymers were loaded individually with isotopically enriched metals 115In (MilliporeSigma), 158Gd (Fluidigm), 163Dy (Fluidigm), 166Er (Fluidigm), and 175Lu (Fluidigm). Metal-loaded polymers were then conjugated to their respective antibodies (Supplemental Tables 1 and 2). 194Pt (Fluidigm) was directly conjugated to the reduced antibody. Antibody concentrations in the wash buffer were quantified using NanoDrop. The final antibody concentrates were then diluted in a stabilization buffer (Candor) containing 0.3% sodium azide. Each antibody was titrated by testing a range of 3–4 serial dilutions to identify the concentration that permits discrimination while minimizing spillover signals. Viability was marked by incubation in palladium chloride (MilliporeSigma) dissolved in DMSO and diluted in PBS to 500 nM for 5 minutes at room temperature. A total of 16 splenocytes samples were stained with either 115In-CD45 or 194Pt-CD45 antibody barcodes (8 each) for 25 minutes at room temperature. One sample from each of the group (vehicle or BAFF) were duplexed together for downstream processing. Each 2-plex sample was blocked with 1 μg anti–mouse Fc block (BD Biosciences) (Supplemental Tables 1 and 2) for 10 minutes at room temperature, followed by a cocktail of surface marker antibodies in cell staining buffers (Fluidigm) at room temperature for 30 minutes. Intracellular cytokine staining was performed using Foxp3 staining kit (eBioscience) per manufacturer's protocol. Upon completion of staining, cells were stored in fresh 1% methanol-free formaldehyde in PBS (Thermo Fisher Scientific) until the day of data collection. Just before data collection, all cells were labeled with rhodium (Fluidigm) at 1:1000 for 45 minutes at room temperature. Mass cytometry

data were acquired at the University of Maryland School of Medicine Center for Innovative Biomedical Resources (CIBR) Flow Cytometry and Mass Cytometry Core Facility (Baltimore, Maryland, USA). Randomization, bead normalization, and bead removal of data collected were performed on CyTOF software (Fluidigm) v6.7. Using FlowJo v10.5, single cell events were identified by gating a tight population based on cell length and rhodium signal. Dead cells were then eliminated by manually gating out cells positive for 106Pd and 108Pd on a biaxial plot. Debarcoding was carried out by manual gating to select for events that are positive for one barcode and negative for other. Analysis was performed using a modified analysis pipeline from Nowicka et al. (47) in R v3.5. FlowSOM algorithm (48) was used to define 20 metaclusters, which were annotated into 8 final immune cell subtypes. These clusters were then visualized using a 2-dimensional uniform manifold approximation and projection (UMAP) dimensional reduction algorithm (49). A total of 2000 random cells per sample was used for visualization.

Construction of a bystander BAFF-secreting cell line for whole-cell BAFF vaccines. We created a 3T3-derived isogenic, stable cell line that constitutively secretes high levels of soluble mouse BAFF under a constitutive promoter, elongation factor 1a (EF1a), using a commercially available vector and host cell system (Flp-In System, Invitrogen). Using this kit, the mus musculus TNFSF13B gene was specifically introduced into the validated FRT locus, simultaneously providing hygromycin resistance. Parental 3T3 cells that did not undergo Flp-In served as a control (3T3-WT). Hygromycin-resistant cells were expanded, and secretion of soluble BAFF from the resultant cell line (3T3-BAFF) but not in the original host 3T3 cell line (3T3-WT) was confirmed by assaying for BAFF in cell culture media by enzyme-linked immunosorbent assay (Abcam Mouse BAFF ELISA Kit [ab119580]) per the manufacturer instructions. The presence of BAFF on 3T3-BAFF cells was separately confirmed by SDS-PAGE using cell lysates (R&D Systems Mouse BAFF AF2106). 3T3-BAFF and 3T3-WT cells were maintained in DMEM (Invitrogen) supplemented with 10% FBS, 1% L-glutamine, and 0.5% penicillin/streptomycin in a humidified atmosphere at 37°C under 5% CO_2.

Immunizations. We investigated the utility of BAFF as a vaccine adjuvant, using the 3T3-BAFF cell line as a bystander cell–based BAFF-secreting vaccine in combination with irradiated autologous tumor cells and the 3T3-WT cell line in combination with irradiated autologous tumor cells as a control. These immunizations were prepared and performed following protocols established for bystander cell lines that secrete GM-CSF (50). The BAFF vaccine consisted of 1×10^6 3T3-BAFF cells and 1×10^6 tumor cells administered s.c. in 3 limb nodal basins after irradiation at 50 Gy. Mock vaccine consisted of 1×10^6 3T3-WT cells and 1×10^6 tumor cells administered s.c. in 3 limb nodal basins after irradiation at 50 Gy. Vaccinations were performed on day 3 following tumor implantation.

B16F10 cells were cultured in DMEM media supplemented with 10% FBS, 1% L-glutamine, and 0.5% penicillin/streptomycin at 37°C under 5% CO_2. B16F10 cells were implanted s.c. at 1×10^4 tumor cells in the hind leg of C57BL/6J mice. Panc02 cells were maintained in DMEM (Invitrogen) supplemented with 10% FBS, 1% L-glutamine, and 0.5% penicillin/streptomycin in a humidified atmosphere at 37°C under 10% CO_2. They were implanted at 5×10^5 tumor cells in the hind leg of C57BL/6J mice. KPC cells were maintained in RPMI 10% FBS, 1% L-glutamine, 1% penicillin/streptomycin, 1% sodium pyruvate (Invitrogen), and 1% nonessential amino at 37°C in 5% CO_2. KPC cells were implanted at 5×10^4 tumor cells in the hind leg of C57BL/6J mice. NT2.5 cells were cultured in RPMI supplemented with 20% FBS, 1.2% HEPES buffer (Thermo Fisher Scientific), 1% L-glutamine, 1% MEM nonessential amino acids (Thermo Fisher Scientific), 0.5% penicillin streptomycin, 1% sodium pyruvate (MilliporeSigma), 0.2% insulin (NovoLog), and 0.02% gentamicin, at 37°C in 5% CO_2. NT2.5 cells were implanted via injection of 5×10^4 cells into the mammary fat pad of 7- to 8-week-old female neu-N mice.

TCGA analysis. Gene-level RNA sequencing (RNAseq) data were downloaded from Genomic Data Commons harmonized data base for 471 melanoma patients from TCGA using the TCGAbiolinks package (v2.13.4) (51). As gene expression, we used fragments per kilobase of transcript per million mapped reads upper quartile (FPKM-UQ) that were log_2 transformed for the further analysis. To investigate whether BAFF expression was associated with a Th1/IFN-γ gene signature, we combined genes from the published Th1 signature from Bindea et al. (52) and genes from IFN-γ signaling pathway from the Reactome database (http://www.reactome.org) (53). We used TNFSF13B gene expression for BAFF and applied the Pearson correlation test to all genes in the Th1/IFN-γ gene signature to get the correlation coefficient and the corresponding P value. The P values were FDR adjusted using Benjamini-Hochberg correction. To test if BAFF expression was associated with patient survival, we used a log-rank test survival analysis (54). Data analysis was performed using R/Bioconductor software (version 3.5.0) with built-in packages and custom routines.

Statistics. For targeted gene expression analysis, statistical significance was determined by nSolver's DE Call function (Nanostring), and adjusted using the Benjamini-Yekutieli correction method. For survival data, results were plotted using a Kaplan-Meier curve, and statistical significance was determined via a log-rank test. Tumor growth data are plotted as mean ± SEM. Unless otherwise noted, differences between 2 groups were tested using unpaired 2-tailed *t* tests using GraphPad Prism 8 (GraphPad Software Inc.). Differences were considered significant when $P < 0.05$. Statistically significant P values are abbreviated as follows: $*P < 0.05$, $**P < 0.01$, $***P < 0.001$, $****P < 0.0001$. All experiments were repeated at least 2 times.

Study approval. All animal studies were reviewed and approved by the Johns Hopkins IACUC and Biohazards Committee (Baltimore, Maryland, USA). Animals were kept in pathogen-free conditions and were treated in accordance with institutional and American Association of Laboratory Animal Committee policies. All efforts were made to limit animal pain and discomfort.

Author contributions

Acknowledgments

Address correspondence to: Elizabeth M. Jaffee, Bloomberg–Kimmel Institute for Cancer Immunotherapy, Johns Hopkins University School of Medicine, Baltimore, 4M07 Bunting Blaustein Cancer Research Building, 1650 Orleans Street, Baltimore, Maryland 21287, USA. Phone: 410.955.2957; Email: ejaffee@jhmi.edu. Or to: Mark Yarchoan, Bloomberg–Kimmel Institute for Cancer Immunotherapy, 1650 Orleans Street CRBI 4M08, Baltimore, Maryland 21287, USA. Phone: 410.955.7141; Email: mark.yarchoan@jhmi.edu.

1. Harris DP, et al. Reciprocal regulation of polarized cytokine production by effector B and T cells. *Nat Immunol*. 2000;1(6):475–482.
2. Lund FE. Cytokine-producing B lymphocytes-key regulators of immunity. *Curr Opin Immunol*. 2008;20(3):332–338.
3. Rock KL, Benacerraf B, Abbas AK. Antigen presentation by hapten-specific B lymphocytes. I. Role of surface immunoglobulin receptors. *J Exp Med*. 1984;160(4):1102–1113.
4. Yan J, Harvey BP, Gee RJ, Shlomchik MJ, Mamula MJ. B cells drive early T cell autoimmunity in vivo prior to dendritic cell-mediated autoantigen presentation. *J Immunol*. 2006;177(7):4481–4487.
5. Hong S, et al. B Cells Are the Dominant Antigen-Presenting Cells that Activate Naive CD4^{+} T Cells upon Immunization with a Virus-Derived Nanoparticle Antigen. *Immunity*. 2018;49(4):695–708.e4.
6. Tullin S, Farris P, Petersen JS, Hornum L, Jackerott M, Markholst H. A pronounced thymic B cell deficiency in the spontaneously diabetic BB rat. *J Immunol*. 1997;158(11):5554–5559.
7. Rivera A, Chen CC, Ron N, Dougherty JP, Ron Y. Role of B cells as antigen-presenting cells in vivo revisited: antigen-specific B cells are essential for T cell expansion in lymph nodes and for systemic T cell responses to low antigen concentrations. *Int Immunol*. 2001;13(12):1583–1593.
8. Hauser SL, et al. Ocrelizumab versus Interferon Beta-1a in Relapsing Multiple Sclerosis. *N Engl J Med*. 2017;376(3):221–234.
9. Hauser SL, et al. B-cell depletion with rituximab in relapsing-remitting multiple sclerosis. *N Engl J Med*. 2008;358(7):676–688.
10. Edwards JC, et al. Efficacy of B-cell-targeted therapy with rituximab in patients with rheumatoid arthritis. *N Engl J Med*. 2004;350(25):2572–2581.
11. Pescovitz MD, et al. Rituximab, B-lymphocyte depletion, and preservation of beta-cell function. *N Engl J Med*. 2009;361(22):2143–2152.
12. McFarland HF. The B cell--old player, new position on the team. *N Engl J Med*. 2008;358(7):664–665.
13. Schwartz M, Zhang Y, Rosenblatt JD. B cell regulation of the anti-tumor response and role in carcinogenesis. *J Immunother Cancer*. 2016;4:40.
14. Helmink BA, et al. B cells and tertiary lymphoid structures promote immunotherapy response. *Nature*. 2020;577(7791):549–555.
15. Cabrita R, et al. Tertiary lymphoid structures improve immunotherapy and survival in melanoma. *Nature*. 2020;577(7791):561–565.
16. Petitprez F, et al. B cells are associated with survival and immunotherapy response in sarcoma. *Nature*. 2020;577(7791):556–560.

17. Mackay F, Schneider P. Cracking the BAFF code. *Nat Rev Immunol*. 2009;9(7):491–502.

18. Mackay F, Browning JL. BAFF: a fundamental survival factor for B cells. *Nat Rev Immunol*. 2002;2(7):465–475.

19. Cambier JC, Gauld SB, Merrell KT, Vilen BJ. B-cell anergy: from transgenic models to naturally occurring anergic B cells? *Nat Rev Immunol*. 2007;7(8):633–643.

20. Mackay F, Sierro F, Grey ST, Gordon TP. The BAFF/APRIL system: an important player in systemic rheumatic diseases. *Curr Dir Autoimmun*. 2005;8:243–265.

21. Groom JR, et al. BAFF and MyD88 signals promote a lupuslike disease independent of T cells. *J Exp Med*. 2007;204(8):1959–1971.

22. Mackay F, Leung H. The role of the BAFF/APRIL system on T cell function. *Semin Immunol*. 2006;18(5):284–289.

23. Steri M, et al. Overexpression of the Cytokine BAFF and Autoimmunity Risk. *N Engl J Med*. 2017;376(17):1615–1626.

24. Mackay F, Schneider P, Rennert P, Browning J. BAFF AND APRIL: a tutorial on B cell survival. *Annu Rev Immunol*. 2003;21:231–264.

25. Shulga-Morskaya S, et al. B cell-activating factor belonging to the TNF family acts through separate receptors to support B cell survival and T cell-independent antibody formation. *J Immunol*. 2004;173(4):2331–2341.

26. Schiött A, Lindstedt M, Johansson-Lindbom B, Roggen E, Borrebaeck CA. CD27- CD4+ memory T cells define a differentiated memory population at both the functional and transcriptional levels. *Immunology*. 2004;113(3):363–370.

27. Robert R, et al. Essential role for CCR6 in certain inflammatory diseases demonstrated using specific antagonist and knockin mice. *JCI Insight*. 2017;2(15):94821.

28. Overacre-Delgoffe AE, Vignali DAA. Treg Fragility: A Prerequisite for Effective Antitumor Immunity? *Cancer Immunol Res*. 2018;6(8):882–887.

29. Koizumi M, et al. Increased B cell-activating factor promotes tumor invasion and metastasis in human pancreatic cancer. *PLoS One*. 2013;8(8):e71367.

30. Sanmamed MF, et al. Agonists of Co-stimulation in Cancer Immunotherapy Directed Against CD137, OX40, GITR, CD27, CD28, and ICOS. *Semin Oncol*. 2015;42(4):640–655.

31. Hollern DP, et al. B Cells and T Follicular Helper Cells Mediate Response to Checkpoint Inhibitors in High Mutation Burden Mouse Models of Breast Cancer. *Cell*. 2019;179(5):1191–1206.e21.

32. Hu X, et al. Landscape of B cell immunity and related immune evasion in human cancers. *Nat Genet*. 2019;51(3):560–567.

33. Sutherland AP, et al. BAFF augments certain Th1-associated inflammatory responses. *J Immunol*. 2005;174(9):5537–5544.

34. Walters S, et al. Increased CD4+Foxp3+ T cells in BAFF-transgenic mice suppress T cell effector responses. *J Immunol*. 2009;182(2):793–801.

35. Kappos L, et al. Atacicept in multiple sclerosis (ATAMS): a randomised, placebo-controlled, double-blind, phase 2 trial. *Lancet Neurol*. 2014;13(4):353–363.

36. Chen X, Jensen PE. The role of B lymphocytes as antigen-presenting cells. *Arch Immunol Ther Exp (Warsz)*. 2008;56(2):77–83.

37. Shurin MR, et al. BAFF and APRIL from Activin A-Treated Dendritic Cells Upregulate the Antitumor Efficacy of Dendritic Cells In Vivo. *Cancer Res*. 2016;76(17):4959–4969.

38. Plummer JR, McGettigan JP. Incorporating B cell activating factor (BAFF) into the membrane of rabies virus (RABV) particles improves the speed and magnitude of vaccine-induced antibody responses. *PLoS Negl Trop Dis*. 2019;13(11):e0007800.

39. Wu CC, et al. Enhanced anti-tumor therapeutic efficacy of DNA vaccine by fusing the E7 gene to BAFF in treating human papillomavirus-associated cancer. *Oncotarget*. 2017;8(20):33024–33036.

40. Kanagavelu S, et al. HIV-1 adenoviral vector vaccines expressing multi-trimeric BAFF and 4-1BBL enhance T cell mediated anti-viral immunity. *PLoS One*. 2014;9(2):e90100.

41. Tertilt C, et al. Expression of B-cell activating factor enhances protective immunity of a vaccine against Pseudomonas aeruginosa. *Infect Immun*. 2009;77(7):3044–3055.

42. Chen L, et al. BAFF enhances B-cell-mediated immune response and vaccine-protection against a very virulent IBDV in chickens. *Vaccine*. 2009;27(9):1393–1399.

43. Ng LG, et al. B cell-activating factor belonging to the TNF family (BAFF)-R is the principal BAFF receptor facilitating BAFF costimulation of circulating T and B cells. *J Immunol*. 2004;173(2):807–817.

44. Sakurai D, Kanno Y, Hase H, Kojima H, Okumura K, Kobata T. TACI attenuates antibody production costimulated by BAFF-R and CD40. *Eur J Immunol*. 2007;37(1):110–118.

45. Ou X, Xu S, Lam KP. Deficiency in TNFRSF13B (TACI) expands T-follicular helper and germinal center B cells via increased ICOS-ligand expression but impairs plasma cell survival. *Proc Natl Acad Sci USA*. 2012;109(38):15401–15406.

46. Tai YT, et al. APRIL signaling via TACI mediates immunosuppression by T regulatory cells in multiple myeloma: therapeutic implications. *Leukemia*. 2019;33(2):426–438.

47. Nowicka M, et al. CyTOF workflow: differential discovery in high-throughput high-dimensional cytometry datasets. *F1000Res*. 2017;6:748.

48. Van Gassen S, et al. FlowSOM: Using self-organizing maps for visualization and interpretation of cytometry data. *Cytometry A*. 2015;87(7):636–645.

49. Becht E, et al. Dimensionality reduction for visualizing single-cell data using UMAP. *Nat Biotechnol*. 2019;37:38–44.

50. Ercolini AM, et al. Recruitment of latent pools of high-avidity CD8(+) T cells to the antitumor immune response. *J Exp Med*. 2005;201(10):1591–1602.

51. Colaprico A, et al. TCGAbiolinks: an R/Bioconductor package for integrative analysis of TCGA data. *Nucleic Acids Res*. 2016;44(8):e71.

52. Bindea G, et al. Spatiotemporal dynamics of intratumoral immune cells reveal the immune landscape in human cancer. *Immunity*. 2013;39(4):782–795.

53. Croft D, et al. Reactome: a database of reactions, pathways and biological processes. *Nucleic Acids Res*. 2011;39(Database issue):D691–D697.

54. Therneau TM. Survival: Survival Analysis. R-Project. https://cran.r-project.org/web/packages/survival/index.html. Published April 10, 2020. Accessed April 24, 2020.